

# The Centrosome Keeps Nucleating Microtubules but Looses the Ability to Anchor Them after the Inhibition of Dynein–Dynactin Complex

O. N. Zhapparova<sup>1,2</sup>, A. V. Burakov<sup>3\*</sup>, and E. S. Nadezhdina<sup>1,3</sup>

<sup>1</sup>*Institute of Protein Research, Russian Academy of Sciences, ul. Institutskaya 4, 142290 Pushchino,  
Moscow Region, Russia; fax: (495) 632-7871; E-mail: elena.nadezhdina@gmail.com*

<sup>2</sup>*Biological Faculty, Lomonosov Moscow State University, 119992 Moscow, Russia;  
fax: (495) 939-4309; E-mail: olga.zhapparova@gmail.com*

<sup>3</sup>*Belozersky Institute of Physico-Chemical Biology, Lomonosov Moscow State University,  
119992 Moscow, Russia; fax: (495) 939-3181; E-mail: antburakov@yandex.ru*

Received April 18, 2007

Revision received June 21, 2007

**Abstract**—We inhibited dynein in cells either by the expression of coiled coil-1 (CC1) fragment of dynactin p150Glued subunit or by the microinjection of CC1 protein synthesized in *Escherichia coli*. CC1 impeded the aggregation of pigment granules in fish melanophores and caused the dispersion of Golgi in Vero and HeLa cells. These data demonstrated the inhibiting effect of CC1 on dynein. In cultured cells, CC1 expression caused the disruption of microtubule array, while the nucleation of new microtubules remained unaltered. This was proved both with *in vivo* microtubule recovery after nocodazole treatment and with *in vitro* microtubule polymerization on centrosomes, when the number of nucleated microtubules marginally reduced after the incubation with CC1. Moreover, the inhibiting anti-dynein 74.1 antibodies caused the same effect. Thus we have shown that though dynein is not important for microtubule nucleation, it is essential for the radial organization of microtubules presumably being involved in microtubule anchoring on the centrosome.

DOI: 10.1134/S0006297907110090

**Key words:** dynein, dynactin, microtubules, centrosome, p150Glued, microinjections, melanophores

The radial array of microtubules organizes intracellular transport and ensures polarization of moving cells. The array radiates from the centrosomal region [1, 2] where new tubules are nucleated, and some of them remain bound (anchored) to the centrosome or to nearby organelles. Minus-ends of anchored microtubules are protected from depolymerization, increasing the pool of polymerized tubulin and thus determining the dynamics of microtubule plus-ends [3]. The molecular mechanisms of microtubule organization on the centrosome remain unclear due to high complexity of the centrosomal components.

The major microtubule-nucleating machines are  $\gamma$ -tubulin ring complexes ( $\gamma$ -TuRCs).  $\gamma$ -TuRCs are attached to the centrosome and consist of several proteins [4, 5]. Some microtubule-anchoring proteins are already known: PCM-1 [6], Cep135 [7], ninein [6, 8], CAP350 and FOP [9], but many others remain obscure. The mechanism of microtubule translocation between nucleating and anchoring complexes is also poorly understood. Also, there might be some other microtubule-nucleating complexes besides  $\gamma$ -TuRCs.

Dynein—a minus-end microtubule motor—is also located on the centrosome, but its functions there remain obscure. Cytoplasmic dynein was shown to nucleate microtubules *in vitro* [10]. It is also essential for centrosome-independent microtubule self-organization in fish melanophores [11, 12]. Moreover, dynein interacts with  $\gamma$ -TuRCs [13] and ninein [8, 14] and delivers them to the

**Abbreviations:** DHC) dynein heavy chain; DIC) dynein intermediate chain; GFP) green fluorescent protein; GST) glutathione-S-transferase.

\* To whom correspondence should be addressed.

centrosome. Thus, dynein might take part in microtubule nucleation and anchoring or it might coordinate the interactions between nucleating and anchoring complexes on the centrosome.

There are several experimental approaches to inhibit dynein and thus reveal its functions on the centrosome. Though specific pharmaceutical agents have not yet been found, dynein activity can be inhibited with monoclonal anti-dynein intermediate chain (DIC) antibodies 74.1 [15]. An alternative approach is the inhibition of dynein–dynactin interactions. Dynactin is a multisubunit cofactor that enhances dynein activity and links it to the transported vesicles and other cargoes [2]. Dynactin is concentrated on the centrosome in animal cells and binds growing plus-ends of microtubules. Dynactin complex consists of p150Glued, dynamitin, Arp1, and some other proteins [2, 16]. The N-terminal part of p150Glued comprises a microtubule-binding domain (amino acids 18–157). Dynein-binding region of p150Glued lies between amino acids 200 and 811, and most of it (amino acids 217–548) is organized into a coiled-coil structure—CC1. The dynein intermediate chain interacts with CC1 via its 1–123 amino acid region [17]. The overexpression of either p150Glued-CC1 or DIC N-terminal fragments entails the dissociation of dynein–dynactin complex and causes the inhibition of dynein activity [17, 18].

The expression of a full-length dynein intermediate chain or its fragment (amino acids 1–237) caused Golgi dispersion in *Dictyostelium* cells [19], indicating the inhibition of dynein-dependent transport. The expression of p150Glued-CC1, fragments of DIC, and some other dynactin-disrupting constructs in mammalian interphase cells also entailed the dispersion of Golgi and the disorganization of microtubule radial array [20]. Moreover, the centrosome activity (estimated by the number of microtubules re-growing from the centrosome after microtubule depolymerization) was also reduced. This suggests that dynein–dynactin complex might play a key role in the radial organization of microtubules in interphase cells [20, 21]. But it still remains unclear whether dynein and dynactin are responsible for the nucleation or for anchoring of microtubules on the centrosome.

We disrupted dynein–dynactin interactions expressing p150Glued-CC1 in cells and observed the system of microtubules to confirm the data published in [20, 21]. We were interested in the alterations of centrosome activity and changes in microtubule organization under dynein inhibition. The experiments were performed on HeLa and Vero cells—two cultured lines that vary in the level of centrosome activity and of microtubule radial organization. Our main goal was to study the influence of recombinant glutathione-S-transferase (GST)-fused p150Glued-CC1 and 74.1 antibodies on the centrosome-induced microtubule growth *in vitro*, i.e. directly on the nucleating activity of the centrosome. Such experiments

had not been performed before and could provide a direct proof whether dynein was essential for microtubule nucleation on the centrosome.

## MATERIALS AND METHODS

Vector pCDNA3Zeo+ containing full-length cDNA of human p150Glued was a kind gift of Prof. W. Steffen. For cDNA cloning, we used primers carrying sites for restriction endonucleases. The primers were from Syntol (Russia). To clone cDNA of p150Glued-CC1 into pEGFP-C2 (Clontech, USA) we used forward (5'-aaagaattcgaggaggactaagggt) and reverse (5'-aaaggtaccaggtggctgctgctgttcct) primers. To clone the interdomain of p150Glued (amino acids 550–923, p150Glued-ID) into the same vector we used forward (5'-ttagaattccagagaccttgactt) and reverse (5'-ttaggtaccccggtggag-gctgtctg) primers (both fragments were cloned on EcoRI and KpnI restriction sites). To clone p150Glued-CC1 cDNA into pGEX-4T3 (GE Healthcare, Great Britain) we used primers 5'-aaagatccgaggaggactaagggt and 5'-aaagtgcacaggtggctgctgttc terminating in sites for BamHI and SalI. Amplification was performed with a GenePak PCR Core reagent kit (Isogene, Russia). Restriction endonucleases and T4 ligase were from Fermentas (Lithuania). DNA constructs were verified with automatic sequencing in a Genome apparatus (Russia). Plasmid DNA was purified with QIAprep Spin Miniprep Kit and EndoFree Plasmid Maxi Kit (Qiagen, USA).

Vero (green monkey kidney epithelia-like cells) and HeLa (human cervical carcinoma) cells were cultured in standard conditions (37°C, in an atmosphere of 5% CO<sub>2</sub>) in medium containing 50% Dulbecco's modified Eagle's medium (DMEM) and 50% F12 (Paneco, Russia), supplemented with 7.5% fetal bovine serum (Serva, USA) and 80 µg/ml gentamicin (Sigma, USA).

To verify that GST-p150Glued-CC1 inhibited dynein, we microinjected p150Glued-CC1 into black tetra melanophores and observed the aggregation of pigment granules—a dynein-dependent process [22]. Melanophores were obtained as described previously [23]. Melanocytes were grown on Petri dishes and on cover-slips for immunofluorescent staining.

Transfection was performed using Unifectin-56 (Unifect, Russia) for HeLa cells and Unifectin-M (Unifect) for Vero cells according to the manufacturer's recommendations. Posttransfection (24 h) cells were fixed with methanol (–20°C) for 5 min, then with 3% paraformaldehyde at 4°C for 15 min, washed three times (for 10 min) with PBS, treated with 0.5% Triton X-100 for 10 min, and immunostained.

For the experiments with tubulin, we used PEM buffer (80 mM PIPES, pH 6.7, 20 mM KCl, 1 mM MgCl<sub>2</sub>, 1 mM EGTA, 0.1 mM EDTA). Microtubules were isolated from either pig or rat brain and tubulin was

purified as described previously [24, 25]. Briefly, microtubules obtained after a cycle of depolymerization/polymerization were suspended in ice-cold 0.5 M PIPES, pH 6.8, containing 20 mM KCl, 1 mM  $MgCl_2$ , 2 mM EGTA, and 1 mM GTP, then clarified by centrifugation, and polymerized again after the addition of 5% dimethylsulfoxide (DMSO) for 30 min at 37°C. Microtubules were sedimented in 4 M glycerol (45 Ti rotor, Spinco L-8 centrifuge; Beckman, USA) at 35,000 rpm for 1 h, dissolved in cold PEM buffer containing 1 mM GTP, and clarified by centrifugation. Then aliquots were frozen in liquid nitrogen.

Recombinant GST-p150Glued-CC1 was isolated from *Escherichia coli* extract on a glutathione-agarose column (Sigma) according to the manufacturer's instructions. To purify GST we used empty pGEX-4T3 vector. Mouse monoclonal 74.1 antibodies (Covance, USA) were purified on protein-A-Sepharose.

For *in vitro* microtubule polymerization, cells were grown on cover slips pretreated with poly-L-lysine. The next day cells were incubated with 2  $\mu$ g/ml nocodazole for 3 h, washed with ice-cold PBS containing 1 mM phenylmethylsulfonyl fluoride (PMSF) and 10  $\mu$ g/ml leupeptin, then treated for 3 min with PEM containing 0.5% Triton X-100 and Complete protease inhibitor cocktail (Roche Applied Science, USA). Permeabilized cells (cell "ghosts") were incubated in a humidified chamber with PEM containing protease inhibitors and either 0.25 mg/ml of 74.1 antibodies or 1 mg/ml of GST-p150Glued-CC1 for 15 min at room temperature. Then the ghosts were incubated in the same solution with 1.2 mg/ml tubulin and 1 mM GTP for 40 min at 37°C, washed with PEM, and fixed in 0.5% glutaraldehyde.

For immunofluorescent staining, we used monoclonal anti- $\alpha$ -tubulin antibodies DM-1A (Sigma), fluorescein isothiocyanate (FITC)-conjugated DM-1A (Sigma), monoclonal anti-p150Glued antibodies (BD Transduction Laboratories, USA), monoclonal anti-dynein heavy chain (DHC) antibodies (Abcam, USA), rabbit anti-mannosidase-II antibodies (Abcam), and anti- $\gamma$ -tubulin antibodies (a generous gift of Prof. R. E. Uzbekov). Tetramethylrhodamine B isothiocyanate (TRITC)-conjugated secondary goat anti-mouse or anti-rabbit antibodies were from Jackson ImmunoResearch (USA). Immunostained cells were visualized with an Axiophot microscope (Zeiss, Germany) equipped with Planaro 63 $\times$  and 40 $\times$  objectives and CCD MicroMax camera (Princeton Instruments, USA).

Electrophoresis and immunoblotting were performed as described previously [24]. Immunoblots were stained with monoclonal anti-GFP (green fluorescent protein) antibodies (Rusbiolink, Russia) and horseradish peroxidase conjugated goat anti-mouse antibodies. Peroxidase was developed in 0.5  $\mu$ g/ml diaminobenzidine and  $H_2O_2$ .

## RESULTS

We first checked whether p150Glued-CC1 fragment influenced dynein-dependent transport. GST-fused p150Glued-CC1 was purified from *E. coli* extract with affinity chromatography on glutathione-agarose. Electrophoresis of the purified GST-p150Glued-CC1 sample revealed that the molecular mass of recombinant protein coincided with the predicted mass (64 kD) and the sample contained mostly the protein of interest (Fig. 1a). Purified GST-p150Glued-CC1 was microinjected

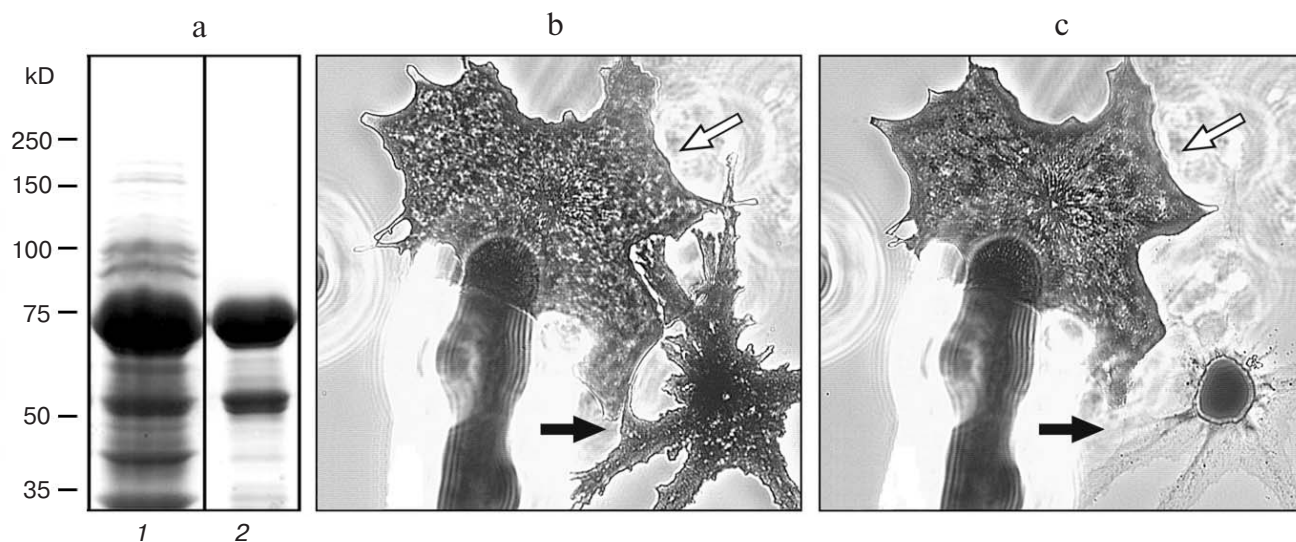


**Fig. 1.** GST-p150Glued-CC1 microinjection inhibits dynein activity in fish melanophores. a) Coomassie-stained gel: 1) total lysate of *E. coli* expressing pGEX-p150Glued-CC1; 2) affinity column-purified GST-p150Glued-CC1 protein. Molecular markers (kD) are indicated. b, c) Aggregation of pigment granules in response to adrenalin. White arrow, GST-p150Glued-CC1-microinjected cell; black arrow, the nearby control cell. Adrenalin was added 30 min after microinjection. b, c) 10 sec and 10 min after adrenalin addition, respectively.

into fish melanophores, whose pigment granules were evenly dispersed in the cytoplasm. The microinjection did not alter the viability of the melanocytes: they remained bound to the substrate and their pigment granules kept moving. Adrenalin treatment of control cells (Fig. 1, b and c, black arrows) caused pigment granule aggregation, whereas in microinjected cells granules remained dispersed (Fig. 1, b and c, white arrows). Since pigment granule aggregation depended on dynein-mediated transport, p150Glued-CC1 inhibited dynein activity in melanocytes. The microinjection of GST did not influence the aggregation of pigment granules (data not shown).

Microtubules in interphase Vero and HeLa cells might be organized either in radial arrays or chaotically. To estimate the level of radial organization, we asked 2-3

experts to evaluate radial organization of microtubules in cells on the photographs. To obtain an objective result the experts did not know which cells (control or treated) they were analyzing. Thus most Vero cells contained a distinct radial array of microtubules with insignificant number of disorganized tubules (Fig. 2, b and d). In HeLa cells, the radial array was not so distinct, its center was unfocused, and only 60% of HeLa cells possessed radially organized microtubules, and in the others microtubules were distributed chaotically (Fig. 2, b and c).

HeLa and Vero cells were transfected with pEGFP-p150Glued-CC1. After transfection (24 h later) cells were either fixed and immunostained with anti-tubulin antibodies or homogenized and subjected to immunoblotting. Immunoblots stained with anti-GFP antibodies revealed a 64 kD GFP-p150Glued-CC1 polypeptide, whose

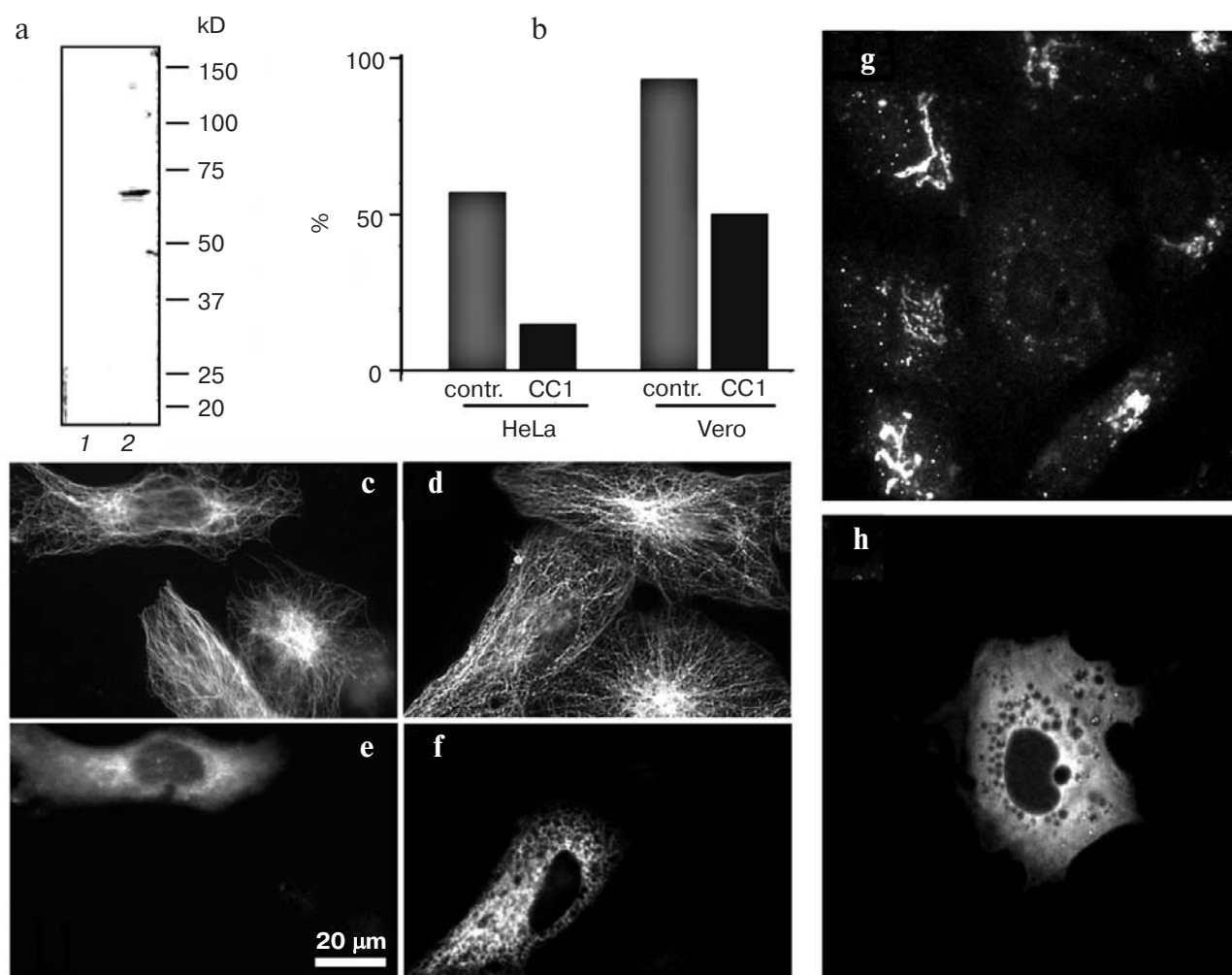


**Fig. 2.** pEGFP-p150Glued-CC1 expression in mammalian cells leads to the dispersion of Golgi (c, f) and disruption of microtubule radial array (g, h). a) Immunoblotting of HeLa cells stained with anti-GFP antibodies: 1) control cells; 2) cells transfected with pEGFP-p150Glued-CC1. Molecular markers (kD) are indicated. b) Percentage of untransfected (control) and pEGFP-p150Glued-CC1-expressing (CC1) HeLa and Vero cells with radial microtubule array. One (of three) representative experiment is shown. Eighty-three (83) and 118 cells were evaluated. c-f) pEGFP-p150Glued-CC1 expression entails microtubule chaotization. c, e) HeLa cells; d, f) Vero cells. c, d) Anti- $\alpha$ -tubulin immunostaining; e, f) GFP fluorescence of the same transfected cells. g, h) pEGFP-p150-CC1 expression causes the dispersion of Golgi in Vero cells. g) Anti-mannosidase II immunostaining; h) GFP fluorescence of the same cells.



molecular mass coincided with the predicted value (Fig. 2a). The radial array of microtubules was disrupted in most Vero cells expressing GFP-p150Glued-CC1: microtubules were evenly distributed in the cytoplasm and their density was not increased in cell center (Fig. 2, d and f). In HeLa cells transfected with GFP-p150Glued-CC1 the radial microtubule system was also damaged: there were no microtubule radiality in most cells (Fig. 2, c and e), though the total number of microtubules (estimated visually) did not change significantly. In control cells expressing GFP-p150Glued-ID, the radial system of microtubules remained unaltered (compared to untransfected cells; data not shown).

Golgi complex in Vero cells visualized with anti-mannosidase-II antibodies usually forms a compact structure located in the perinuclear region (Fig. 2g). In cells expressing GFP-p150-CC1, Golgi was dispersed and its small vesicles were randomly distributed in the cytoplasm (Fig. 2, g and h). This proved the inhibition of dynein activity under GFP-p150-CC1 expression.

To reveal whether GFP-p150-CC1 affects nucleating or anchoring activity of the centrosome, we studied the recovery of microtubules after their depolymerization. Vero cells transfected with either pEGFP-p150-CC1 or pEGFP-p150-ID were treated with 3  $\mu$ g/ml of nocodazole for 3 h and washed with medium at 37°C. At 3 min after nocodazole wash-out, all control and transfected cells formed asters of short microtubules radiating from the centrosome (Fig. 3, a and d). Ten minutes later, the asters remained but their microtubules grew longer,

reaching the cell periphery (Fig. 3, b and e). After 1 h of nocodazole wash-out we detected a peculiarity of cells expressing GFP-p150-CC1: the microtubule system lost its radiality and became chaotic, while in wild-type and GFP-p150-ID-expressing control cells it remained radial (Fig. 3, c and f). Thus, we found that in cells expressing p150-CC1 the centrosome kept nucleating microtubules but lost the ability to anchor them for a long time.

Furthermore, to discover the role of dynein in centrosome-mediated nucleation of microtubules we studied the influence of anti-dynein 74.1 antibodies and GST-p150Glued-CC1 on *in vitro* polymerization of microtubules on centrosomes. Cells with nocodazole-depolymerized microtubules were permeabilized with Triton X-100 and cell ghosts were pre-incubated either with control buffer, 74.1 antibodies, or GST-p150Glued-CC1, and then incubated with tubulin at 37°C, fixed, and immunostained for microtubules (Fig. 4a). It was critical to set tubulin concentration so that microtubules would grow only on the centrosome, but not throughout the solution. The sample of purified tubulin contained mostly the protein of interest with an insignificant amount of contaminating proteins that were hardly seen even on the overloaded gel (Fig. 4b). The optimal tubulin concentration was approximately 1.2 mg/ml, which is consistent with other authors' data [26]. Higher concentrations of tubulin resulted in the appearance of free microtubules, which made it difficult to observe the centrosome-bound ones (data not shown). At 1.2 mg/ml of tubulin, microtubules radiated from the centrosome and only individual

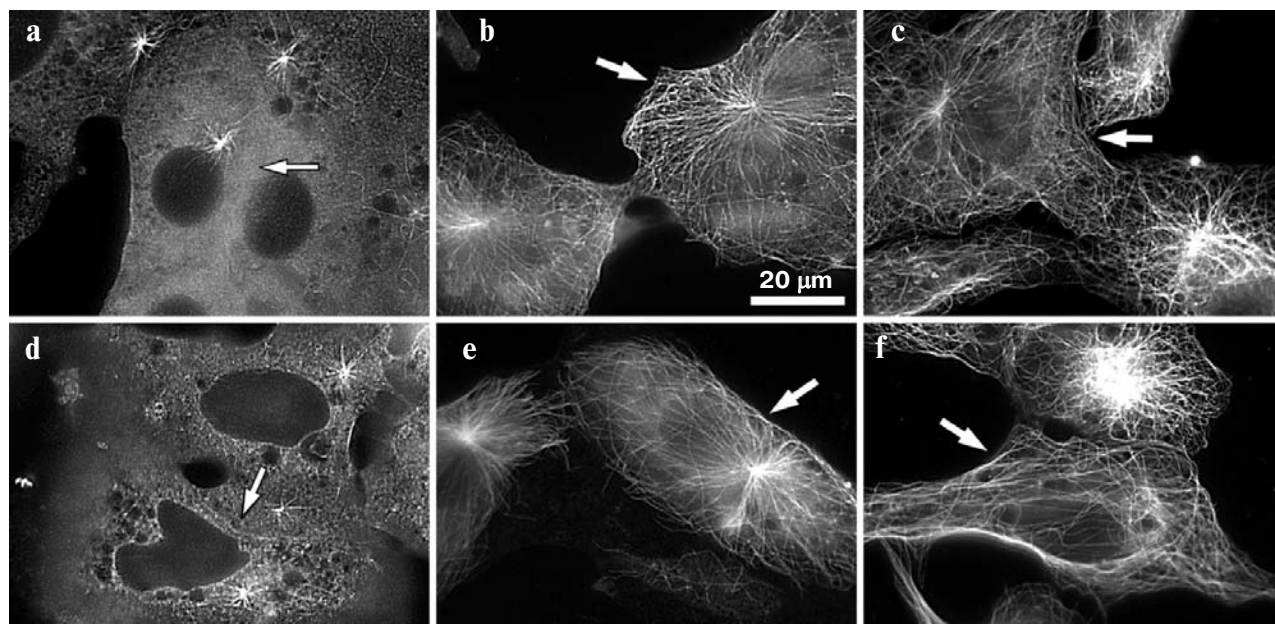


**Fig. 3.** GFP-p150-CC1 expression impairs centrosome functions but does not affect the microtubule-nucleating activity. Microtubules regrowth after nocodazole-induced depolymerization at 37°C. a–c) pEGFP-p150-ID expression; d–f) pEGFP-p150-CC1 expression (transfected cells are indicated with arrows). a, d) 3 min; b, e) 10 min; c, f) 1 h of nocodazole wash-out. Cells transfected with pEGFP-p150-ID or pEGFP-p150-CC1 form asters of microtubules, but GFP-p150-CC1 eventually causes the disruption of radial array.

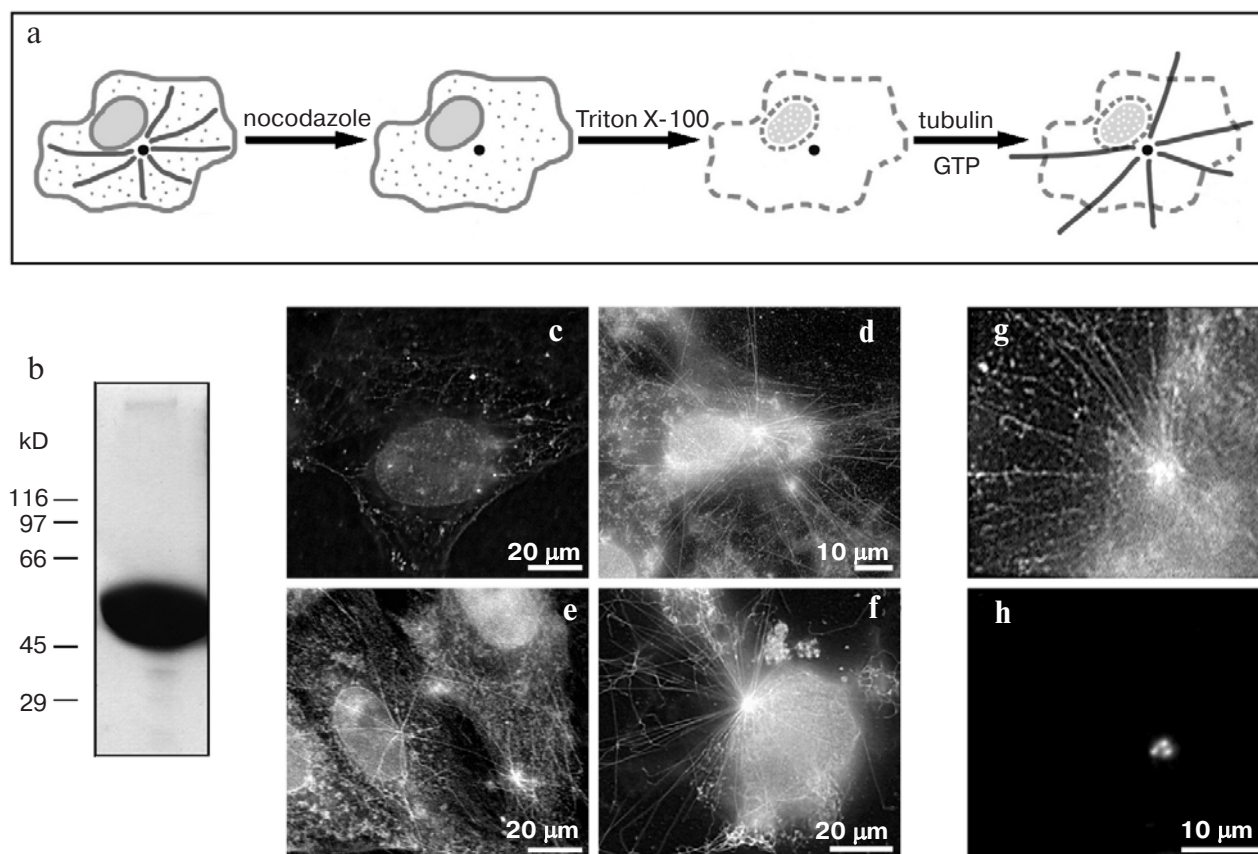


**Fig. 4.** The centrosome keeps nucleating microtubules *in vitro* under the inhibition of dynein. a) Scheme of *in vitro* microtubule polymerization on the centrosome. b) Tubulin isolated from pig brain (Coomassie staining). Molecular markers (kD) are indicated. c-f) Microtubule polymerization in cell ghosts: c) cell ghosts incubated with tubulin-free buffer; d-h) cell ghosts incubated with tubulin form asters of microtubules radiating from the centrosome: e, f) cell ghosts preincubated with 74.1 antibodies and GST-p150-CC1, respectively. g, h) Centrosome in cell ghosts double stained with anti- $\alpha$ - and  $\gamma$ -tubulin antibodies. c-g) Anti- $\alpha$ -tubulin immunostaining; h) anti- $\gamma$ -tubulin immunostaining. In all experiments microtubules were organized in asters radiating from the centrosome.

ones were not bound to it (Fig. 4d). The centrosome was visualized by  $\gamma$ -tubulin staining (Fig. 4, g and h). Cell ghosts incubated in tubulin-free buffer contained single residual microtubules, but microtubule asters were never observed (Fig. 4c).

For the experiments with 74.1 antibodies, we used tubulin from pig brain stored in liquid nitrogen. After the incubation with tubulin, 93% of cell ghosts formed a radial aster of microtubules around the centrosome. Each aster contained approximately  $14.7 \pm 4.3$  microtubules (minimum 7, maximum 27). The number of nucleated microtubules slightly decreased after the incubation with 74.1 antibodies: 68% of cells formed radial asters containing approximately  $11.7 \pm 5.1$  microtubules (minimum 4, maximum 26), i.e. 80% compared to the control (Fig. 4e). Thus, 74.1 antibodies significantly but slightly inhibited microtubule-nucleating activity of the centrosome ( $p = 0.0004$ ).

For the experiments with GST-p150-CC1 we used tubulin freshly prepared from rat brain. After the incubation with this tubulin 79% of cell ghosts formed radial

arrays, containing more microtubules than in the experiments with pig brain tubulin: each aster was composed of  $39.4 \pm 15.3$  microtubules (minimum 15, maximum 64). The incubation with GST-p150-CC1 did not affect aster formation: 80% of cells formed radial arrays of  $31.3 \pm 8.9$  microtubules (minimum 21, maximum 48), i.e. 79.5% compared to the control (Fig. 4f). Thus, GST-p150-CC1 slightly inhibited microtubule-nucleating activity of the centrosome ( $p = 0.03$ ), as in case of 74.1 antibodies.

To confirm that centrosomes in cell ghosts contained dynein and dynactin, we immunostained them with 74.1, anti-DHC, and anti-p150Glued antibodies. Cellular ghosts were fixed before the incubation with tubulin, and the centrosome was visualized with anti- $\gamma$ -tubulin antibodies. Both dynein and dynactin remained bound to the centrosome after nocodazole and Triton X-100 treatment (Fig. 5). Unfortunately, we could not confirm it with immunoblotting as antibody staining revealed the indicated proteins also in the nuclei. Thus, both dynein and dynactin might influence microtubule assembly on the centrosome in our *in vitro* experiments.

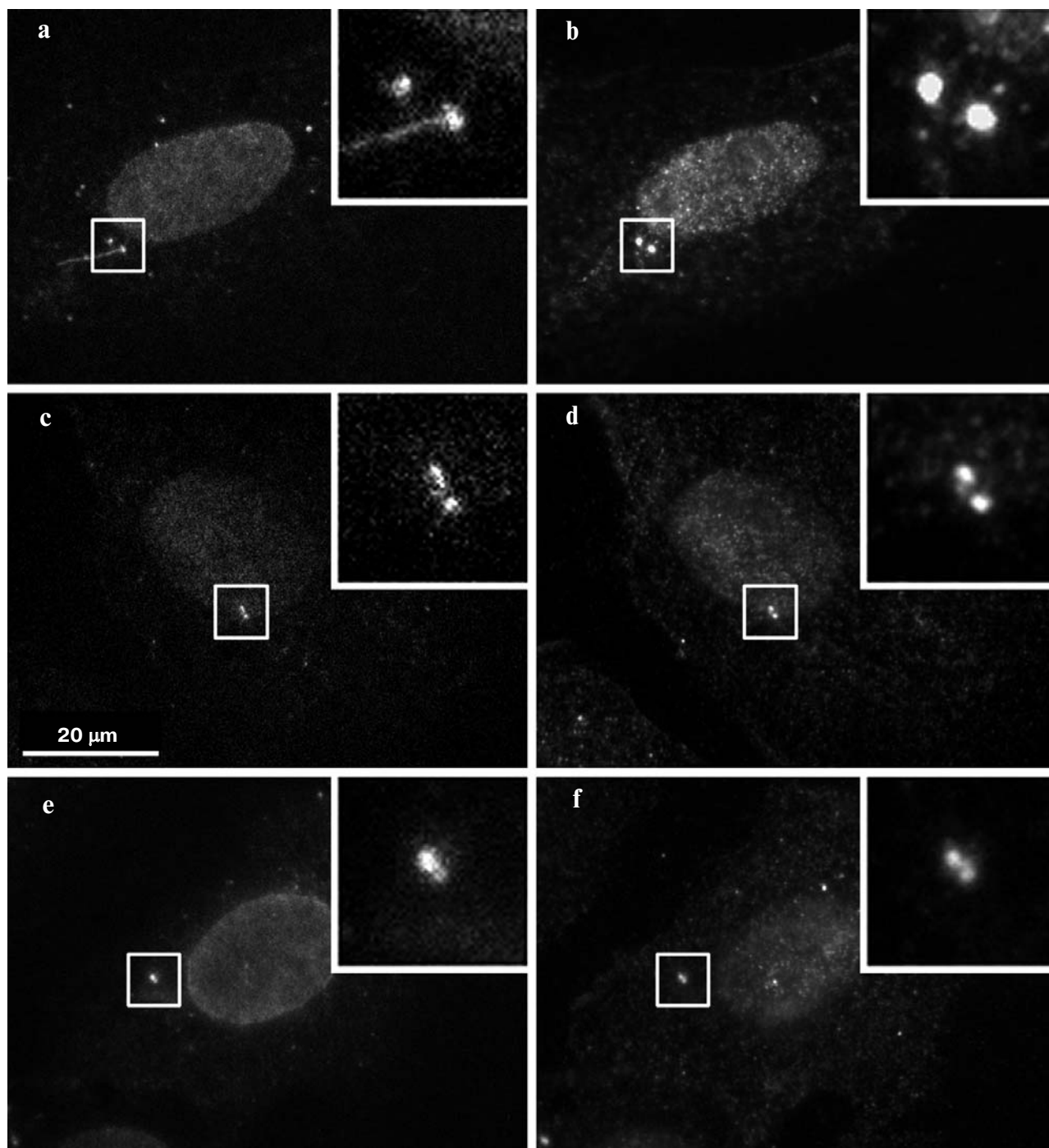


**Fig. 5.** Centrosomes of cell ghosts contain dynein and dynactin. Double immunostaining with anti- $\gamma$ -tubulin (b, d, f) and 74.1 (a), anti-DHC (c) or anti-p150Glued (e) antibodies. Boxed regions are shown in insets with higher magnification.

## DISCUSSION

Dynein is responsible for microtubule minus-end directed intracellular transport, i.e. for the aggregation of pigment granules in fish melanophores [22] and for the compact organization of Golgi [27]. We microinjected

GST-p150-CC1 into fish melanocytes and observed a specific inhibition of pigment granule aggregation. This data proved that GST-p150-CC1 inhibited dynein activity. This p150Glued fragment had never been used to inhibit granule movement in melanocytes, though a similar effect was observed with 70.1 antibodies [28] that had



the same dynein-inhibiting activity as 74.1 ones. Another evidence of dynein inhibition was the dispersion of Golgi in Vero cells expressing p150Glued-CC1. A similar effect of dynein inhibition to Golgi localization has been reported in other works (for review see [16]).

Our experiments with p150-CC1 expression confirmed the works of other authors: radial arrays of microtubules were disorganized in most transfected cells. This effect was observed both in Vero cells, where microtubules were usually organized in distinct radial arrays, and in HeLa cells with their low-focused radiality and low activity of the centrosome. Similar data—chaotization of microtubules in 60–70% cells—were obtained previously in Cos7 cultured cells [20].

Our main goal was to determine whether dynein inhibition disrupted microtubule-nucleation activity of the centrosome and thus affected radial organization of microtubules. We demonstrated that dynein-inhibiting agents did not significantly alter the nucleating activity of centrosome either *in vivo* or *in vitro* and the centrosome could organize microtubules in radial array for short periods of time. Thus, dynein–dynactin complex is not essential for microtubule nucleation on the centrosome, though it is able to nucleate tubules *in vitro* [10]. Presumably the inhibition of dynein–dynactin interactions affects the anchoring of microtubules on the centrosome [13, 17, 20, 21, 29]. The chaotization of microtubules might also result from the dispersion of Golgi, which is known to contribute to microtubule organization in cells [2]. It is also possible that dynein translocates microtubules from nucleating to anchoring complexes on the centrosome.

The authors are grateful to R. E. Uzbekov and W. Steffen for antibodies and cDNA, to V. I. Rodionov for melanocytes, and to N. A. Shanina for fruitful discussions.

This work was financially supported by the Program of Presidium of the Russian Academy of Sciences “Molecular and Cellular Biology”, Russian Foundation for Basic Research (grant No. 05-04-49015), and FIRCA (grant RC1-2400-MO-02).

## REFERENCES

- Gould, R. R., and Borisy, G. G. (1990) *J. Cell Biol.*, **73**, 601–613.
- Burakov, A. V., and Nadezhdina, E. S. (2006) *Ontogenez*, **37**, 1–17.
- Rodionov, V., Nadezhdina, E., and Borisy, G. (1999) *Proc. Natl. Acad. Sci. USA*, **96**, 115–120.
- Moritz, M., Braunfeld, M., Sedat, J., Alberts, B., and Agar, D. (1995) *Nature*, **378**, 638–640.
- Dictenberg, J., and Zimmerman, W. (1998) *J. Cell Biol.*, **141**, 163–174.
- Dammermann, A., and Merdes, A. (2002) *J. Cell Biol.*, **159**, 255–266.
- Uetake, Y., Terada, Y., Matulienė, J., and Kuriyama, R. (2004) *Cell Motil. Cytoskeleton*, **58**, 53–66.
- Delgehyr, N., Sillibourne, J., and Bornens, M. (2005) *J. Cell Sci.*, **118**, 1565–1575.
- Yan, X., Habedanck, R., and Nigg, E. A. (2006) *Mol. Biol. Cell*, **17**, 634–644.
- Malikov, V., Kashina, A., and Rodionov, V. (2004) *Mol. Biol. Cell*, **15**, 2742–2749.
- Rodionov, V., and Borisy, G. (1997) *Nature*, **386**, 170–173.
- Vorobjev, I., Malikov, V., and Rodionov, V. (2001) *Proc. Natl. Acad. Sci. USA*, **98**, 10160–10165.
- Young, A., Dictenberg, J. B., Purohit, A., Tuft, R., and Doxsey, S. J. (2000) *Mol. Biol. Cell*, **11**, 2047–2056.
- Casenghi, M., Barr, F. A., and Nigg, E. A. (2005) *J. Cell Sci.*, **118**, 5101–5108.
- Dillman, J. F., 3rd, and Pfister, K. K. (1994) *J. Cell Biol.*, **127**, 1671–1681.
- Schroer, T. (2004) *Annu. Rev. Cell Biol.*, **20**, 159–179.
- King, S., Brown, C., Kerstin, C., Quintyne, N., and Schroer, T. (2003) *Mol. Biol. Cell*, **14**, 5089–5097.
- Burkhard, J., Echeverri, C., Nilsson, T., and Valee, B. (1997) *J. Cell Biol.*, **139**, 469–484.
- Ma, S., and Trivinos-Lagos, L. (1999) *J. Cell Biol.*, **147**, 1261–1273.
- Quintyne, N. J., Gill, S. R., Eckley, D. M., Crego, C. L., Compton, D. A., and Schroer, T. A. (1999) *J. Cell Biol.*, **147**, 321–334.
- Quintyne, N., and Schroer, T. (2002) *J. Cell Biol.*, **159**, 245–254.
- Rodionov, V. I., Hope, A. J., Svitkina, T. M., and Borisy, G. G. (1998) *Curr. Biol.*, **8**, 165–168.
- Gyoeva, F. K., Leonova, E. V., Rodionov, V. I., and Gelfand, V. I. (1987) *J. Cell Sci.*, **88**, 649–655.
- Shanina, N. A., Ivanov, P. A., Chudinova, E. M., Severin, F. F., and Nadezhdina, E. S. (2001) *Mol. Biol. (Moscow)*, **35**, 638–646.
- Castoldi, M., and Popov, A. V. (2003) *Protein Expr. Purif.*, **32**, 83–88.
- Kuriyama, R. (1984) *J. Cell Sci.*, **66**, 277–295.
- Harada, A., Takei, Y., Kanai, Y., Tanaka, Y., Nonaka, S., and Hirokawa, N. (1998) *J. Cell Biol.*, **141**, 51–59.
- Nilsson, H., and Wallin, M. (1997) *Cell Motil. Cytoskeleton*, **38**, 397–409.
- Fumuto, K., Hoogenraad, C. C., and Kikuchi, A. (2006) *EMBO J.*, **25**, 5670–5682.